EUR 490.e

EUROPEAN ATOMIC ENERGY COMMUNITY - EURATOM

A STUDY ON THE PERFORMANCE OF NEUTRON BEAM EXPERIMENTS AT THE PULSED FAST REACTOR SORA

by

R. HAAS and H. B. MØLLER

1963

Joint Nuclear Research Center
Ispra Establishment - Italy

Reactor Physics Department
Experimental Neutronics Service

LEGAL NOTICE

This document was prepared under the sponsorship of the Commission of the European Atomic Energy Community (EURATOM).

Neither the EURATOM Commission, its contractors nor any person acting on their behalf :

1° — Make any warranty or representation, express or implied, with respect to the accuracy, completeness, or usefulness of the information contained in this document, or that the use of any information, apparatus, method, or process disclosed in this document may not infringe privately owned rights ; or

2° — Assume any liability with respect to the use of, or for damages resulting from the use of any information, apparatus, method or process disclosed in this document.

The authors' names are listed in alphabetical order.

This report can be obtained, at the price of Belgian Francs 85,— from : PRESSES ACADEMIQUES EUROPEENNES — 98, Chaussée de Charleroi, Brussels 6.

Please remit payments :

— to BANQUE DE LA SOCIETE GENERALE (Agence Ma Campagne) — Brussels — account No 964.558,

— to BELGIAN AMERICAN BANK AND TRUST COMPANY — New York — account No 121.86,

— to LLOYDS BANK (Foreign) Ltd. — 10 Moorgate — London E.C.2,

giving the reference : « EUR 490 . e — A study on the performance of neutron beam experiments at the pulsed fast reactor SORA ».

This document was duplicated on the basis of the best available copy.

Printed by IMPRIMERIE L. VANMELLE, S.A., GHENT.
Brussels, December 1963.

E U R 4 9 0 . e

A STUDY ON THE PERFORMANCE OF NEUTRON BEAM EXPERIMENTS AT THE PULSED FAST REACTOR SORA
by R. HAAS and H. B. MØLLER

European Atomic Energy Community — EURATOM
Joint Nuclear Research Center
Ispra Establishment (Italy)
Reactor Physics Department
Experimental Neutronics Service
Brussels, December 1963 — Pages 63 — Figures 6

The performance of pulsed neutron beam experiments is analyzed for its efficiency at a pulsed fast reactor. The assumed reactor characteristics are : mean power 100(250)kW, pulse width 50 μsec, pulse frequency 12.5(100)sec^{-1} and a background power of 20 % mean power.

It is found that a double chopper and a rotating crystal spectrometer, which cover the neutron energy range from 1 mev to about

E U R 4 9 0 . e

A STUDY ON THE PERFORMANCE OF NEUTRON BEAM EXPERIMENTS AT THE PULSED FAST REACTOR SORA
by R. HAAS and H. B. MØLLER

European Atomic Energy Community — EURATOM
Joint Nuclear Research Center
Ispra Establishment (Italy)
Reactor Physics Department
Experimental Neutronics Service
Brussels, December 1963 — Pages 63 — Figures 6

The performance of pulsed neutron beam experiments is analyzed for its efficiency at a pulsed fast reactor. The assumed reactor characteristics are : mean power 100(250)kW, pulse width 50 μsec, pulse frequency 12.5(100)sec^{-1} and a background power of 20 % mean power.

It is found that a double chopper and a rotating crystal spectrometer, which cover the neutron energy range from 1 mev to about

500 mev, compare well with the instrumentation, which is likely to be installed at a Very High Flux Reactor (for instance the 100 MW ENEA project). The expected low background for the measurements and the low cooling power for a cold source are interesting features.

The intensity obtained by a fast chopper is compared with that of a Lineac for key neutron cross section measurements. An equal performance is found for both.

General requirements for the reactor operation, reactor shielding and the beam hole design are given.

Finally, the thermal neutron flux as a function of time in a small moderator is estimated.

500 mev, compare well with the instrumentation, which is likely to be installed at a Very High Flux Reactor (for instance the 100 MW ENEA project). The expected low background for the measurements and the low cooling power for a cold source are interesting features.

The intensity obtained by a fast chopper is compared with that of a Lineac for key neutron cross section measurements. An equal performance is found for both.

General requirements for the reactor operation, reactor shielding and the beam hole design are given.

Finally, the thermal neutron flux as a function of time in a small moderator is estimated.

EUR 490.e

EUROPEAN ATOMIC ENERGY COMMUNITY - EURATOM

A STUDY ON THE PERFORMANCE OF NEUTRON BEAM EXPERIMENTS AT THE PULSED FAST REACTOR SORA

by

R. HAAS and H. B. MØLLER

1963

Joint Nuclear Research Center
Ispra Establishment - Italy

Reactor Physics Department
Experimental Neutronics Service

C O N T E N T S

A STUDY ON THE PERFORMANCE OF NEUTRON BEAM EXPERIMENTS AT THE PULSED FAST REACTOR S O R A

A b s t r a c t

The performance of pulsed neutron beam experiments is analyzed for its efficiency at a pulsed fast reactor. The assumed reactor characteristics are : mean power 100(250) kW, pulse width 50 μsec, pulse frequency 12.5(100) sec^{-1} and a background power of 20% mean power.

It is found that a double chopper and a rotating crystal spectrometer, which cover the neutron energy range from 1 mev to about 500 mev, compare well with the instrumentation, which is likely to be installed at a Very High Flux Reactor (for instance the 100 MW ENEA project). The expected low background for the measurements and the low cooling power for a cold source are interesting features.

The intensity obtained by a fast chopper is compared with that of a Lineac for kev neutron cross section measurements.
An equal performance is found for both.

General requirements for the reactor operation, reactor shielding and the beam hole design are given.

Finally, the thermal neutron flux as a function of time in a small moderator is estimated.

1.- INTRODUCTION.

In the present report we will give the main design characteristics for experimental equipment for neutron research using neutron beams from the pulsed fast reactor "SORA". For the purpose of this study its operating characteristics are assumed to be :

mean power	$\bar{P}$	=	100 kW
peak power	P_{max}	=	120 MW
minimum power (constant)	P_{min}	=	20 kW
pulse frequency	ν_r	=	12.5 sec^{-1}
half-width of pulse	w	=	50 μsec

Different operating characteristics will be discussed in chapter 5.
The following types of apparatus will be considered :

1) Double choppers
2) Rotating crystal spectrometer
3) Fast chopper

The first two instruments will be used for solid and liquid state research in the subthermal, thermal, and epithermal energy region, and the last instrument for total cross section measurements in the kev energy region.
For each of these instruments the intensity and resolution will be estimated and a comparison with similar instruments operating at "Very High Flux Reactors" or Linear Accelerators will be made.
In chapter 5 we arrive at conclusions and recommendations concerning the reactor operation and design.

2.- APPARATUS FOR NEUTRON ENERGIES SMALLER THAN 1 EV.

In this section we will develop instruments for the epithermal, thermal and subthermal energy region. All instruments considered employ

necessarily pulsed neutron techniques. They are designed to allow the measurement of neutron-scattering as a function of energy and scattering angle.

To obtain the respective neutron beams we must place a moderator into the fast reactor. Due to the long lifetime of the thermal neutrons in this scatterer, the thermal neutron pulse width gets still wider (100 μsec). If pulses of this width are used, one has to have very long flight paths, to obtain a reasonable resolution. It is therefore more convenient (and it gives also more intensity) to use only part of the neutron pulse from the moderator. This shortening of the neutron pulse can be done by the use of a slow chopper or a rotating crystal and this leads to the double chopper instrument or rotating crystal spectrometer.

2.1.- DOUBLE CHOPPERS.

In order to obtain a pulsed beam of monochromatic thermal or subthermal neutrons a double chopper can be used at the SORA reactor. The choppers are designed to pulse thermal neutrons only, because the fast neutrons from the reactor pulse are eliminated by the timing or by a Be-filter. The experimental set-up is shown in fig.1.

Two conventional slow choppers are used with a set of parallel curved slits to give a large beam area and maximum transmission for the selected neutron velocity v_n. The geometric beam area is always $a_2 \times b_2$ (5×10 cm^2). However F_2 (cm^2) is the effective beam area taking the finite absorber between slits into account ($t = 0.05$ cm).

The radius of curvature ρ is determined by the wellknown relation :

$$v_n = 4\pi\nu\rho$$

where ν is the rotational frequency of the chopper. The neutron velocities of the upper and lower cut-offs are :

$$v_1 = v_n / (1 + \beta)$$

$$v_2 = v_n / (1 - \beta) \quad \text{with } \beta = 2\varrho\, s/r^2$$

where s is the width of one slit and 2r is the diameter of the chopper. If β is larger than unity, there is no upper cut-off. However, the chopper delivers a second burst per revolution with a lower cut-off :

$$v'_2 = v_n / (\beta - 1)$$

The fight time over the flight path l_2 (cm) of the "right" neutrons, the slowest neutrons and the fastest neutrons respectively transmitted by the first chopper are :

$$t_2 = \frac{l_2}{v_n}$$

$$t_2^s = \frac{l_2}{v_n} \quad (1 + \beta)$$

$$t_2^f = \frac{l_2}{v_n} \quad (1 - \beta)$$

In order to avoid overlap between successive neutrons bursts of the first chopper during the burst time of the second chopper the following condition must be satisfied (since $\sqrt{\Delta t^2 + \Delta t_s^2} \ll \beta t_2$, see also below) :

$$t_2^s \leq t_2 + \frac{1}{\nu_r}$$

or

$$t_2 \beta \leq \frac{1}{\nu_r}$$

where ν_r is repetition rate of the reactor pulses.

The half width of the neutron pulse for a parallel beam is

$$\Delta t = \frac{s}{4\pi \nu r}$$

The fact that the neutron beam is not exactly parallel collimated introduces a widening Δt_s of the neutron pulse which is determined by the sweeptime through the angle α_2.

$$\Delta t_s = \frac{a_2}{2\pi\nu\, l_2}$$

For the SORA reactor set up α_2 is given by $\alpha_2 = \frac{a_2}{l_2}$

If Δt_s is of the same size as Δt the resolution of the incoming and scattered neutron beams are respectively

$$\frac{\Delta E_1}{E_1} = 4\,\frac{\Delta t}{t_2}$$

$$\frac{\Delta E_2}{E_2} = 2\sqrt{2}\,\frac{\Delta t}{t_3}$$

If Δt_s is much smaller than Δt the resolutions are

$$\frac{\Delta E_1}{E_1} = 2\sqrt{2}\,\frac{\Delta t}{t_2}$$

$$\frac{\Delta E_2}{E_2} = 2\,\frac{\Delta t}{t_3}$$

where t_3 is the flight time over the analyzing flight path l_3. We have neglected the finite size of the sample, the distance between second chopper and sample, and the thickness of the detector.

The number of neutrons falling on the sample per sec is

$$I_2 = \frac{F_2}{4\pi (l_1 + l_2)^2}\,(1 + A + B + AB)\;\Delta t \nu_r \phi(E)\Delta E_1$$

where

$$A = \begin{cases} \left(\frac{a_1}{a_2} - 1\right)\left(1 + \frac{l_2}{4l_1} - \frac{l_2}{4l_1}\frac{a_1}{a_2}\right) & \text{for } a_2 \leq a_1 \leq \frac{2l_1 + l_2}{l_2}\, a_2 \\ \frac{l_1}{l_2} & \text{for } \frac{2l_1 + l_2}{l_2}\, a_2 \leq a_1 \end{cases}$$

and the analogue expression for B.

For the SORA double choppers, here considered, we have in all cases

$$A = \frac{l_1}{l_2} \quad \text{and} \quad B = 0$$

which gives

$$I_2 = \frac{F_2^2}{4\pi l_2 (l_1 + l_2)}\, \Delta t\, \nu_r\, \phi(E)\, \Delta E_1$$

The number of neutrons incident on the counter bank per sec is

$$I_3 = I_2\, R_s\, \frac{F_3}{4\pi l_3^2}$$

where R_s is the fraction of the neutrons scattered isotropically from the sample $F_3/(4\pi l_3^2)$ is the solid angle of the counter bank and ε its efficiency.

Tables 1 and 2 show, how the various dimensions of choppers and flight paths can be chosen to give double chopper arrangements covering the energy range from ~1mev to ~80mev. For each energy we consider an energy resolution of incoming as well as scattered neutron energies between ~1% and ~10%.

The countrate I_3 is calculated in terms of the neutron flux within the energy range accepted by the double chopper.

We have assumed R_s to be 0.1 and we have adjusted the area F_3 of the counter bank se that the relative solid angle $F_3/(4\pi l_3^2)$ is always 2×10^{-4}. We have considered elastic scattering only and adjusted l_3 to give the wanted energy resolution of the scattered neutron beam.

The collimations of incident and scattered neutron beams are calculated from

$$\alpha_2 = \frac{a_2}{l_2}$$

$$\alpha_3 = \frac{\sqrt{F_3}}{l_3}$$

2.2.- ROTATING CRYSTAL SYSTEM.

The pulsed reactor allows the installation of a fixed crystal spectrometer as a pulsed beam monochromator.

But rotation of the crystal provides a possibility to suppress higher order reflections (because of the different arrival times of the neutrons at the outer end of the beam tube) and to shape the neutron pulse in a very easy way.

This instrument may also be designed as fixed crystal plus chopper. For the general discussion here, this version is considered identical with the above one.

Fig. 2 shows the set-up.

F_1 is the radiating area at the scatterer ; F_2 is the beam area which is accepted by the monochromator crystal. F_3 represents the sensitive counter area which is limited in size so that the solid angle for the analyzer path stays constant.

The distance between monochromator crystal and sample is considered negligible, since the beam collimation and resolution are quite good. It is assumed that the sample intercepts the whole neutron beam.

From the operational point of view, the instrument consists of two independent parts, the monochromator and analyzer.

The energy set by the monochromator depends on the angle of diffraction θ and the interplanar spacing d :

$$2d\sin\theta = \lambda = \frac{0,28}{\sqrt{E}} \qquad d\,[\text{Å}]\,,\quad E\,[\text{ev}]$$

The resolution is given by :

$$\frac{\Delta E_2}{E_2} = 2\,\text{ctg}\,\theta\,\Delta\theta$$

or

$$\Delta\theta = 0,5\,\frac{\Delta E_2}{E_2}\,\text{tg}\,\theta$$

Table 3 shows the situation for different θ angles, and different interplanar distances d, using a Soller slit collimator $\Delta\theta = 0,5 \times 10^{-2}$.

Completely independent from this part is the analyzer. The resolution may be defined as $\frac{\Delta E_3}{E_3} = 2\,\frac{\Delta t}{t_3}$

The burst time required is therefore

$$\Delta t = \frac{1}{2}\,\frac{\Delta E_3}{E_3}\,\frac{l_3}{v_3}$$

and the speed of the rotation of the crystal

$$n = \frac{\Delta\theta}{\Delta t} \times \frac{60}{2\pi} \approx 10\,\frac{\Delta\theta}{\Delta t} \qquad \text{rpm}$$

as example :

from $v_3 = 2000$ m/sec, $\frac{\Delta E_3}{E_3}$ 2.5 10^{-2}, $l_3 = 4$m and $\Delta\theta = 10^{-2}$ rad

follows $\Delta t = 25$ sec

$n = 4 \times 10^3$ rpm

The countrate at the counterbank may be calculated as follows

$$I_3 = \frac{F_1 F_2}{4\pi l_2^2} \frac{\Delta\theta}{\alpha_2} R_m R_s \frac{F_3}{4\pi l_3^2} \nu_r \Delta t \phi(E)\Delta E \varepsilon$$

$F_1 = F_2 = 25$ cm^2, $l_2 = 200$ cm, $\frac{F_3}{4\pi l_3^2} = 2 \times 10^{-4}$

α_2 = beam divergence without Soller collimator: $\alpha_2 \frac{5}{200} = 25 \times 10^{-3}$

$\frac{\Delta\theta}{\alpha_2}$ = reduction because of Soller collimator.

R_M = crystal reflectivity = 0.5

R_S = fraction of isotropically scattered neutrons = 0.1

ν_r = pulse frequency of the reactor = 12.5 sec^{-1}

ε = efficiency of the counterbank = 1.0

Δt = burst time actually accepted by the instrument (sec)

$\phi(E)\Delta E$ = neutron flux at the scatterer for energies between E and E + E.

With the above numbers the formula reduces to

$$I_3 = 1.6 \times 10^{-7} \frac{\Delta\theta}{\alpha_2} \Delta t \phi(E)\Delta E$$

or, as a function of the actual resolutions :

$$I_3 = 1.6 \times 10^{-6} \frac{\Delta E_2}{E_2} \frac{\Delta E_3}{E_3} \operatorname{tg} \theta \frac{l_3}{\sqrt{3}} \phi(E) \Delta E$$

Table 4 gives a set of intensity values for different energies and resolutions for elastic scattering and

$$\frac{\Delta E_2}{E_2} = \frac{\Delta E_3}{E_3}$$

Two facts should be noted :

The intensities are proportional to l_3 (calculations are for $l_3 = 4$ m) as long as the corresponding Δt does not exceed the width of the pulse at the scatterer (~ 100 μ sec).

The intensities also increase for larger θ angles (that means for smaller interplanar distances of the crystal), as long as $\Delta\theta$ does not exceed α_2 :

For $v_n = 4000$ m/sec, $2\theta = 90°$ ($\operatorname{tg}\theta = 1.0$, d = 0.7 Å), $\Delta\theta = \alpha_2 = 2{,}5 \times 10^{-2}$, the count rate is increased in all 3 cases by a factor of 3, if the crystal can still be chosen to have 50 % reflectivity and for n = 10000 rpm

For $v_n = 1100$ m/sec, $2\theta = 126°$ ($\operatorname{tg}\theta = 2$, d = 1 Å), $\Delta\theta = \alpha_1 = 5 \times 10^{-2}$

($F_1 = 10 \times 10$ cm^2, $F_2 = 25$ cm^2, $l_2 = 200$ cm),

the countrate is increased by a factor of 4 (in both cases of table 4).

Note : If the reflecting crystal is mounted on its rotating support in such a way, that different sets of planes get into reflecting position during one revolution, the energy can be changed in discret steps by an adjustment of the phase angle between the reactor pulsation and the crystal only.

2.3.- CONCLUSIONS.

From the description of the double chopper instrument and the rotating crystal spectrometer it is seen that the double chopper gives approximately a factor of two higher intensity for the same resolution. At very low neutron energies only the double chopper can be used, whereas at high energies the rotating crystal spectrometer may be more convenient, because very long flight paths are required for the double chopper.

3.- APPARATUS FOR THE KeV ENERGY REGION.

In this section we investigate the possibilities to use the SORA reactor for total cross section measurements in the kev-region. To obtain the required resolution it is again necessary to use a pulse width much smaller than the width of the reactor pulse, therefore a fast chopper is necessary.

3.1.- FAST CHOPPER.

The design characteristics of a fast chopper operating at the SORA reactor would probably be as follows :

Diameter	$D = 2R$	$= 70$ cm
Slit width	s	$= 1$ mm
Spacer thickness	d	$= 1$ mm
Rotational frequency	ν	$= 200$ sec^{-1}
Number of slits	N_s	

Since the reactor has a duty cycle of less than 200 sec^{-1}, the chopper has only one set of slits.

As the thickness of the material in the beam, right after the transmission of the pulses, is

$$D_{eff} = \frac{dD}{s+d} = 0.5\ D$$

The chopper may be cigar shaped with a long axis D (parallel to the slits) and with a short axis of D_s = Deff + N_s s in order to give constant absorption.

Furthermore, the reactor is "shut down" after 50 μ sec.
During this time the chopper rotates through

$$\alpha = 2\pi\nu W = 0.06 = 3.50^{\circ}$$

The "shut down" reactor has a power of

$$P_{min} = P_{max} / p = 1.6 \times 10^{-4} P_{max} \quad \text{(see table 9)}$$

Therefore the chopper might still be thinner at tight angles to the long axis to permit a transmission which is 6200 times larger than that of the thickness D_s.

These facts permit an economical and safe design of the rotor, which would otherwise be difficult to achieve, owing to the large number of parallel slits.

The pulse width is :

$$\Delta t_p = \frac{s}{4\pi r \nu} \sim 1\ \mu\text{sec}$$

With

flight path l = 1000 m
channel width Δt_D = 1 μsec

this gives the following resolution for 1 kev neutrons ($v_n = 4.5 \times 10^5$ m/sec)

$$\frac{\Delta E}{E} = 2\sqrt{\left(\frac{\Delta t_p}{\Delta t}\right)^2 + \left(\frac{\Delta t_D}{\Delta t}\right)^2} = 2\sqrt{2}\ \frac{t_p}{l}\ v = 1.25 \times 10^{-3}$$

Let us assume here that, due to the cigar shape of the chopper, we are able to have 10 slits 5 cm high.
This gives a beam area F_1 = 5 cm^2.

Let us choose a counter bank of area $F_2 = 1\ m^2$

If boron loaded liquid scintilators are used we can have an efficiency for 1 kev neutrons of $\varepsilon = 0.5$.

The total count rate at the counterbank is

$$I = \phi(E)\,\Delta E\,\frac{F_1 F_2}{4\pi l^2}\,\nu_r\,\Delta t_p\,\varepsilon$$

$$= 2.5 \times 10^{-12}\,\phi(E)\,\Delta E \quad n/sec$$

Overlap of neutrons from successive reactor pulses is no problem. The flight time of 1 kev neutrons over 1 km flight path is ~2msec and the time between successive pulses is

$$\frac{1}{\nu_r} = 80\ m\ sec$$

so overlap neutrons would have to travel 1 km in 82 msec and would therefore have the velocity 12000 m/sec but neutrons of such low velocity are not transmitted by the chopper, its lower cut off being

$$v_c = \frac{2\pi\nu R^2}{s} = 1.5 \times 10^5\ m/sec$$

for straight slits.

If the chopper has the slits curved to give optimum transmission for 1 kev neutrons, their curvature is

$$\rho = \frac{v_n}{4\pi\nu} = 175\ m$$

In this case the lower cut off is

$$v_c = \frac{v_n}{1 + \frac{2\rho s}{R^2}} = 1.1 \times 10^5\ m/sec$$

These neutrons travel 1 km in about 10 msec.

4.- COMPARISON OF THE SORA INSTRUMENTS WITH OTHER SIMILAR INSTRUMENTS.

In the last chapter we developed experimental apparatus for the SORA reactor and found their intensities in terms of flux within the energy range accepted by the monochromator. We now want to compare these instruments with similar instruments, using other types of neutrons sources. We will compare with a "Very High Flux Reactor" (the ENEA project) for the thermal and subthermal energy region and with a linear accelerator (proposed by Poole, Harwell) for the kev region.

4.1.- COMPARISONS IN THE SUBTHERMAL ENERGY REGION.

For the cold energy region where a cooled beryllium filter can be used, we will assume that the fast neutron background is low enough to permit the use of thermal choppers only also for the Very High Flux Reactor. Therefore, for this energy region, we can use the same type of rotors as discussed for the SORA reactor (see Fig.1). The only difference which we assume is, that we are not able to place the first chopper as close to the cold neutron source as was possible at the SORA reactor. In fact it seems practically impossible to place the first chopper close to the source due to the high radiation field and other inherent difficulties. Probably we must have a distance of $l = 400$ cm between cold source and first chopper. We assume the radiating surface of the cold source to be lo x lo cm^2.

In this case the sweeptime must be calculated from.:

$$\Delta t_s = \frac{a_1 + a_2}{4\pi\nu(l_1 + l_2)}$$

and the time between successive neutron pulses is $1/\nu$ sec.

The formula for the neutron intensity at the sample becomes in this case

$$I_2 = \frac{F_2^2}{4\pi(l_1+l_2)^2} \quad (1 + A)\Lambda\, t\nu\phi(E)\Delta E$$

The collimation of the incoming neutron beam is

$$\alpha_2 = \frac{a_1 + a_2}{2(l_1 + l_2)}$$

All other formulae are the same as for the SORA-choppers.

Table 5 gives the design characteristics and intensities for double choppers for the cold energy region.

The thermal flux in the Very High Flux Reactor is (see references)

$$\phi_{th}^{VHFR} \approx 2 \times 10^{15} \quad \frac{n}{cm^2\ sec}$$

The presence of the cold scatterer in the D_2O reflector causes only an insignificant flux depression as shown in appendix I.
The thermal flux for the SORA reactor is shown in appendix II to be

$$\phi_{th}^{SORA} \approx 1.0 \times 10^{15} \quad \frac{n}{cm^2\ sec}$$

The instruments for the Very High Flux Reactor therefore have a factor of 2 more intensity at the source for the thermal and subthermal energy region.

Table 6 gives the ratios of intensities for the VHFR-instrument to the intensities for the SORA instrument for various resolutions.
It is seen that the SORA instrument has almost an order of magnitude lower intensity than similar instruments in operation at the Very High Flux Reactor would have. The SORA instruments are relatively better at limited resolution (short flight paths) where the gain due to the larger solid angle used, is largest. If however the mean power $\bar{P}$ of the SORA

reactor is increased to 250 kW, the situation is improved substantially.

4.2.- COMPARISONS IN THE THERMAL ENERGY REGION.

Here we cannot use a beryllium filter, so we will have an appreciable fast background from the Very High Flux Reactor. It is therefore necessary to operate "fast neutron choppers" in addition to the two thermal choppers. Therefore the simple instrument which was described for the SORA reactor cannot be used for a "Very High Flux Reactor".

An instrument which includes "fast neutron" rotors is in operation at the NRU-reactor (called Four-Rotor-Spectrometer). We take the two thermal choppers from this instrument for our comparison, because the fast choppers are used only to remove fast neutrons and do not influence the thermal beam.

Characteristic data for the thermal choppers are :

diameter	2r	= 25.4 cm
slit width	s	= 0.635 cm
spacer thickness	d	= 0.635 cm
slit height		= 3.2 cm
number of slits	Ns	= 3
maximum rotational frequency	ν	= 600 sec^{-1}

We assume a 10 x 10 cm^2 radiating source surface. The sweeptime is calculated from $\Delta t_s = \frac{a_1 + a_2}{4\pi\nu(l_1 + l_2)}$

and the time between successive neutron pulses is $1/\nu$ sec

The formula for the neutron intensity becomes

$$I_2 = \frac{F_2^2}{4\pi(l_1 + l_2)^2} (1 + A)^2 \Delta t \nu \Phi(E) \Delta E_1$$

The collimation of the incoming neutron beam is

$$\alpha_2 = \frac{a_0 + a_2}{2\,(l_0 + l_2)}$$

All other formulae are the same as for the SORA reactor (see 2.1.-)

Table 7 gives the design characteristics and intensities for a four rotor spectrometer for thermal neutrons.

Table 8 compares the intensities of SORA-instruments and VHFR-instruments for various resolutions.
The intensity at the source is a factor of 4 higher for the VHFR-instruments.

It is seen that for a mean power $\bar{P}$ = 250 kW of the SORA reactor, the instruments compare very well.

4.3.- COMPARISONS IN THE KEV ENERGY REGION.

We compare the SORA fast chopper with linear accelerators for total cross section measurements at 1 kev neutron energy and will for this comparison choose a linac which can be built using well understood technology.

Such an accelerator has according to Poole the following characteristics:

electron energy	100 MeV
peak current	2 A
pulse repetition rate	200 sec^{-1}
max. pulse length	5 μsec
peak neutron output	5 x 10^{17} n/sec

With 5 cm moderator this gives at 1 kev 2.5 x 10^{13} $\frac{n}{cm^2\ sec}$ per kev at the moderator surface.
If this linac is used with a pulse width of 0.25 μsec the flight path must be 250 meters to give the same resolution as the SORA chopper considered above (3.1.-).

We can use boron loaded liquid scintilators of thickness 2,5 cm and with efficiency of 50%, without limiting the resolution.
The flight time of 1 kev neutrons over the 250 meter flight path is 0,57 msec.
The time between successive pulses is 5 msec,
so the overlap neutrons have the velocity

$$\frac{250}{5.57 \times 10^{-3}} \text{ m/sec} = 4,5 \times 10^{4} \text{ m/sec}$$

which corresponds to 10ev neutron energy.

To eliminate these neutrons from the neutron beam one can use a filter of natural boron, which has 37,5 b cross section for 10 ev neutrons and 6,4 b for 1000 ev neutrons. If this filter is chosen to give 50% transmission of 1000 ev neutrons, the transmission of 10 ev neutrons is 1,7% If a larger attenuation of the overlap neutrons is needed one can either choose a thicker filter or use boron enriched in $_5B^{10}$.

Assuming small samples (< 5 cm^2) and 1m^2 counter bank, the total count rate at the counter bank is

$$I = \phi(E)\Delta E \; \frac{5 \times 10^{4}}{4\pi \; 25000^2} \; 200 \; 0.25 \; 10^{-6} \; 0.5 \; 0.5$$

$$= 8 \times 10^{-11} \phi(E)\Delta E \quad \text{n/sec}$$

Since $\frac{\Delta E}{E} = 1,25 \times 10^{-3}$ we have $\Delta E = 1.25$ ev

which gives

$$\phi(E).\Delta E = 3.13 \times 10^{10} \frac{n}{cm^2 \text{ sec}}$$

Insertion of this gives

LINAC : $I = 2.5$ n/sec

For the SORA + fast chopper we found the intensity (3.1)

$$I = 2.5 \times 10^{-12} \phi(E) \Delta E \quad n/sec$$

A flux calculation done for the SORA reactor at 120 MW constant power gave, using the idealized geometry shown in fig.4, appendix II

$$7.6 \times 10^{14} \frac{n}{cm^2 \, sec}$$ in the energy group from 0,454 KeV to 3,00 KeV

for a waterscatterer of 2,32 thickness, placed in the stainless steel reflector at the interface to the blanket.
The flux is 1/E so the flux per kev at 1 kev is

$$\frac{7.6 \times 10^{14}}{\ln \frac{3}{0,455}} = 4.0 \times 10^{14} \frac{n}{cm^2 sec}$$

The intensity for $\frac{\Delta E}{E} = 1,25 \times 10^{-3}$ is therefore

SORA : $I = 2.5 \times 10^{-12} \times 4.0 \times 10.^{14} \times 1.25 \times 10^{-3} = 1.25$ n/sec

which is a factor of 2 less than for the Linac.

However an increase of the mean power of SORA to $\bar{P} = 200$ kW or a reduction of the pulsewidth to w = 25 /sec would compensate for this factor. Since this countrate depends sensitively on the SORA characteristics, we rewrite it in a normalized way :

$$\text{SORA} : I \frac{n}{sec} = 1.25 \frac{\bar{P}}{100} \times \frac{\bar{W} \nu_r}{1200 \times 12.5}$$

$\bar{P}$ = mean reactor power (kW)

$\bar{W}$ = Pmax /$\bar{P}$

$_r$ = reactor frequency

5.- DISCUSSION AND RECOMMENDATIONS.

The comparison of SORA instruments with other high performance instruments has shown clearly that the SORA reactor is a very good source of neutrons for pulsed beam experiments. We have used the operating characteristics for SORA quoted in chapter 1. There is however the possibility to change these parameters. For the comparison (chapter 4) we considered already an increase of the mean power to $\ddot{P} = 250$ kW.

In the following we discuss how the pulse length and frequency should be chosen to optimize the reactor performance for beam experiments.

Finally we summarize the requirements on the reactor design.

5.1.- PULSE LENGTH AT THE SCATTERER.

The discussion of the different experimental facilities has shown that the pulse width at the scatterer is a critical quantity for both the resolution and the intensity. There are 4 main ways to handle this pulse time.

5.1.1.- SHORTENING OF REACTOR PULSE.

If the pulse width of the reactor is shortened, of course keeping the mean power constant, the peak flux is increased since the energy per pulse only depends on the frequency. Therefore a shorter pulse represents a real power increase for all experiments which make use of part of the reactor pulses only and at the same time deal with neutrons which have a lifetime shorter than the reactor pulse length. This is true for epithermal and fast neutrons, if a hydrogeneous scatterer is used. If the pulse width of the reactor is reduced to $W = 25$ µsec the given intensities for the fast chopper and for the epithermal region (rotating crystal) are doubled. For thermal and cold neutrons the burst time in the scatterer depends on the diffusion time in the scatterer, which is long compared to the reactor pulse (~ 50/usec). Therefore no significant

change in flux can be produced by a variation of the reactor pulse length (see appendix II and table 9).

5.1.2. SHORTENING OF THE THERMAL NEUTRON PULSE BY POISONING OR LEAKAGE.

In combination with 5.1.1. these means seem useful for very low energy neutron work. It is seen however in appendix II that the neutron life time should always be larger than the reactor burst time in order not to sacrifice too much peak flux. Since the acceptable burst times are practically always much smaller than the reactor pulse (50 /usec) it is only the peak flux obtainable, which is of interest. Moreover the only reason to use this method would be to eliminate the first chopper of the double chopper equipment. Therefore this method is not useful except for work with cold neutrons (500 m/sec) and bad resolution (100 /usec pulse acceptable, see table 1). In the contrary all means to raise the life time should be used in order to obtain the largest possible peak flux (no poisoning, reflector around the sample).
It may be noted that sorrounding the moderator partly or completely with Be-reflector gives an improvement for both thermal and cold neutrons, if a relatively small moderator is used. In this way a preferred direction of leakage or a preferred energy range of the leaking neutrons is obtained.

The condition that the life time must be shorter than the interval between two reactor pulses places no restriction on the frequency ν_r up to 100 sec^{-1}.

5.1.3.- SHORTENING OF THE ACCEPTED PULSE WIDTH BY USE OF A SLOW CHOPPER

The burst time of neutrons with energies below the Cd-cut off can easily be controlled by a slow chopper. The introduction of such an instrument into a loading hole which intercepts the beam tube at right angles close to the scatterer (50 cm distant) should not present difficulties. (2.1)

5.1.4.- SHORTENING OF THE ACCEPTED PULSE WIDTH BY USE OF A ROTATING CRYSTAL

The rotating crystal spectrometer presents the easiest possibility to modify the pulse width. There is no difference in pulsing at the crystal or right at the scatterer.(2.2)

5.2.- REPETITION RATE OF THE REACTOR

So far the reactor frequency has always been chosen as $\nu_r = 12.5\ sec^{-1}$. In order to find the most suitable frequency, we have to investigate several effects:

The overlap problem constitutes a definitely upper limit, $\nu_r = 100\ sec^{-1}$ (5.2.2.). Countrate considerations favour this upper limit (5.2.1). The evaluation of the background problem suggests strongly a lower ν_r (5.2.3). In principle the range $12.5 \leq \nu_r \leq 100\ sec^{-1}$ fits the general requirements. If possible from the reactor operation point

of view this whole range of ν_r should be made available.

5.2.1. - COUNTRATES

The countrate per burst is: (see tables 1,2 and 4)

$$i_3 = f \phi_{th} \frac{I_3}{\phi(E)\,\Delta E} \cdot \frac{1}{\nu_r}$$

Where f is defined as:

$$f = \frac{\int_{E}^{E+\Delta E} \phi(E)\,dE}{\int_{0}^{\infty} \phi(E)\,dE}$$

In order to evaluate the highest possible countrate per burst, we choose the double chopper, thermal energies and 5% resolution. With $f = 0.02$, $\phi_{th} = 1 \times 10^{15} \frac{n}{cm^2\ sec}$ (see Appendix II), $\nu_r = 12.5 sec^{-1}$ and table 2 we find :

$$i_3 = 13.5 N_{burst}$$

With the mean reactor power raised to 250 kW we arrive at:

$$i_3 = 34\ /_{burst}$$

So far the relative solid angle was taken to be 2×10^{-4} for reasons of comparisons between different kinds of instruments. Since the flight paths involved are not very long, the counter banks may be much larger from the point of view of practical design. The Egelstaff four-rotor-machine uses a relative solid angle of 7×10^{-4} (divergence $\alpha_3 = 0.093$ in

both directions). In many cases the counterbanks may be still larger in the direction perpendicular to the scattering plane. For the moment we will decide on a relative solid angle of 8×10^{-4}. This leads to the following sizes of counterbanks :

$$\left.\begin{array}{lll} l_3 = 2\ m & F = 400\ cm^2 = 20 \times 20\ cm^2 & \\ l_3 = 3\ m & F = 900\ cm^2 = 30 \times 30\ cm^2 & \\ l_3 = 4\ m & F = 1600\ cm^2 = 40 \times 40\ cm^2 & \end{array}\right\} \alpha_3 = 0.1 = 5.7°$$

In our case we arrive at 130 counts per burst and per counter bank for efficiency 1 and 12.5 pulses per second, and 250 kW average power. For elastic and quasi-elastic scattering we run into dead time problems for to-day commercial analyzers (dead time per registered count = 16 /usec). The problem gets still worse if several counter banks are used simultaneously, because the dead times in a subgrouped analyzer add.

Nevertheless with conventional electronics the last problem can be solved. If the reactor frequency is increased to $\nu_r = 100\ sec^{-1}$ we obtain 17 counts per pulse. For elastic scattering experiments the beam size or counter angle should be decreased to obtain no more than ~1 count/pulse. For inelastic scattering the cross sections are so small that no dead time problems occur.

It is seen from the tables of instrumental transmission (tables 1, 2 and 4) that i_3 decreases as neutron energy increases, on the other hand $\phi(E)dE$ decreases towards both sides of the maximum of the Maxwellian distribution for constant resolution. Both decrease with better resolution.

We conclude therefore that no higher repetition rate of the reactor than $\nu_r = 100\ sec^{-1}$ is necessary for thermal neutron work. For work with epithermal and fast neutrons frequencies down to $\nu_r = 12.5\ sec^{-1}$ can be accepted.

5.2.2.- OVERLAP NEUTRONS.

For the double chopper and the rotating crystal overlap may occur both in the analyzer and monochromator part. But due to the travel time in either part (see tables 1, 2, 4) and the monochromating qualities of the slow choppers no such overlap occurs up to reactor frequencies $\nu_r = 200\ \text{sec}^{-1}$.

But for the analyzer part, the main problem is the fast reactor pulse. This neutron burst comes both through the beam hole and the reactor shielding.
This fast pulse arrives at t_f after the monochromatic neutrons reach the sample.

$$\Delta t_f = \frac{\tau}{\nu_r} - t_{max} \quad \text{with} \quad t_{max} = \left(\frac{l_1 + l_2}{v_n} \right)_{max}$$

Double chopper $t_{max} = 4$ m sec

Rotating crystal $t_{max} = 2$ m sec

Since Δt_f cannot be zero for all experiments simultaneously it should be long enough that the whole measurement is finished when the fast neutrons from the following pulse arrive.

For $\nu_r = 100\ \text{sec}^{-1}$ we get $t_f = 6$ msec for the double chopper and 8 msec for the rotating crystal. This is sufficient.
A higher repetition rate of the reactor would yield too short a time for the analyzer part (for thermal and cold neutrons).
Otherwise we would have to shield for the power peak of the reactor. This has to be avoided, because the reactor shield as well as the instrumental shielding in this case would get too large.

The fast chopper passes, at the lower cut off, neutrons of the speed

$$v_n = 10^5 \text{ m/sec}$$

Therefore, for $l = 1$ km there is no frame overlap up to $\nu_r = 100\ \text{sec}^{-1}$.

5.2.3.- POWER RATIO OF THE REACTOR.

We investigate here the problems, which arise from the finite reactor power between pulses, P_{min}. We call the ratio between peak power and minimum power p :

$$p = P_{max} / P_{min}$$

The ratio between peak flux and minimum flux in the scatterer for epithermal and fast neutrons is f_e, for thermal and cold neutrons f_{th}, see appendix II :

$$f_e = p$$

$$f_{th} = p/4 \quad \text{for} \quad w = 50 \ \mu\text{sec}$$

The value p depends on the reactor frequency ν_r and on the pulse width w. Characteristic values are given in table 9.

P_{min} constitutes a background and we are concerned here with the part which comes through the beam hole only.

The relative background is reduced at a smaller ν_r for the following reason :

the counts per analyzer channel and second are independent of ν_r, while the total counting time per channel is proportional to ν_r.

Since the repetition rate of the instruments is higher than the reactor frequency we get "background pulses" at the sample and for the double chopper in addition a constant fast background, when operated without Be filter. We evaluate the situation for all three instruments.

5.2.3.1.- FAST CHOPPER.

The proposed fast chopper delivers 400 pulses/sec. The spacing of these

pulses is $\tau = 2.5 \times 10^{-3}$ sec. For a flight path of length l there is a neutron velocity v_1 of the first pulse ; which overlaps with the velocity v_2 of the second pulse.

$$v_2 = \frac{v_1}{1 - \tau v_1 / l}$$

there is no overlaping for $v_1 \geq l/\tau$

$$\text{or} \quad v_1 \geq 4 \times 10^5 \text{ m/sec}$$

With reference to 3.1 we conclude that there is no overlap for the main pulses up to $\nu_r = 100 \text{ sec}^{-1}$, but main and background pulses do overlap for energies just below kev (see 5.2.3.4.).

5.2.3.2.- ROTATING CRYSTAL SPECTROMETER.

The minimum number of possible reflections seen from the sample are two per revolution (see 2.2.) or 200 burst/sec. There will not be an overlap of these 200 burst/sec (= 5×10^{-3} sec) even for the lowest energy (1000 m/sec) and $l_3 = 4$ m. However, if more than 2 reflections per revolution are available, there will be a definite overlap problem (see note of 2.2.).
Besides that, the presence of the constant power background produces higher orders, even though at a much reduced intensity. The usual ratio of first to second order is increased by the flux ratios f_{th} and f_e respectively given in table 9. This is still good for $\nu_r = 100 \text{ sec}^{-1}$ but for this experiment a lower reactor frequency would be more favorable (see 5.2.3.4.).

5.2.3.3.- DOUBLE CHOPPER.

Here we have two kinds of background : a constant fast one which is not sufficiently attenuated by the slow choppers (for work without Be filter)

and in cases where the repetition rate is higher han the reactor frequency, there is also a pulsed background which may cause difficulties.

It is recalled that a slow chopper operating at 12000 rpm with $\beta \geq 1.0$ delivers 400 bursts/sec (see 2.1.). A system of two such choppers may become extremely involved (as an evaluation of table 2 for v_n = 4000 m/sec shows), if no additional means are taken for the correction of these effects. For $v_n \ll 4000$ m/sec the requirement $\beta \geq 1.0$ can easily be met, in order not to have overlap in the monochromator path.

It remains still to correct for the higher repetition rate in case t_3 is larger than the instrument period ($t_3 = t_2$ for most cases) and to cut down the constant epicadmium background (see 5.2.3.4.).

5.2.3.4.- ROTATING COLLIMATOR.

A simple rotating collimator could be used in combination with the fast chopper, the double chopper and the rotating crystal in order to cut away background pulses and constant epicadmium background.

A tentative specification for this rotor is :

halfwidth of the pulse	= 1 msec
diameter	= 20 cm
speed	= 3000 rpm
slit width	= 6 cm

5.3.- REACTOR SHIELDING.

Throughout this discussion it is assumed that the reactor is well shielded for neutrons and γ-rays for the mean power (up to 250 kW).

5.3.1.- SHIELDING FOR PEAK POWER.

Since the monochromatic neutrons of the double chopper and the rotating crystal spectrometer arrive at the sample between 4 msec and 0,25 msec after the reactor pulse (see tables 1, 2 and 4), the neutrons of the burst, which leak through the shield, should have died away 0,25 msec after the pulse (for epithermal neutron work). This condition can be fulfilled in the following way :

> The maximum slowing down time to thermal energies in the reactor shield should be no longer than 0,25 msec. (this implies hydrogen in the shield). The remaining thermal background can easily be handled.

5.3.2.- LOW POWER SHIELDING.

The average power between 2 reactor pulses P_{min} is about 20% of the mean reactor power $\bar{P}$. If the reactor were shielded for P_{min} only the signal to background ratio were better than at a conventional reactor by the factor p (see table 9).

If the SORA reactor is shielded for the mean power, this factor of merit is improved to be

$$f = \frac{P_{max}}{P_{min}} \quad \frac{\bar{P}}{P_{min}} = 5\,p$$

This factor is valid for epithermal and fast neutron work. For thermal neutron work it has to be divided by 4 (see 5.2.3.).

It is assumed that the experimental facilities are well shielded and do not produce background themselves.
It is seen that for background-reasons a low repetition rate of the reactor is desirable (as previously stated, see 5.2.3.).

It should be pointed out in this connection that the background usually limits the success of low intensity measurements. Therefore the advantage of the considerably lower background (for comparable experiments) at the SORA reactor should be made fully effective for the experiments. The experimenter may decide if he wants to sacrifice part of this advantage to use less shielding of the counter-banks. (light experimental set-up).

5.3.3.- REACTOR HALL.

The wall of the experimental hall should be designed in a way to give no late back scattering of neutrons from the reactor pulse to the experimental set-ups (no moderation: no H_2O in the wall material).

5.3.4.- GAMMA FLUX.

From the experimental point of view there are no recommendations on the γ-shielding. Most of the γ-background arrives prompt (prompt fission γ, capture γ) and for the constant background BF_3- or He^3 - counters for neutron detection are not sensitive.

If γ-measurements are done, or if scintillation methods are employed for neutron detection, the reactor shielding never can meet all the necessary requirements.

5.4.- BEAMHOLE REQUIREMENTS.

There are certain requirements which all beamholes have to fulfill independently of the type of instruments they are intended for. Besides, there are additional requirements for the beamtubes, which depend upon the type of apparatus.

5.4.1.- GENERAL REQUIREMENTS.

All beam tubes must be stepped, having a larger diameter at the outer surface of the reactor. This prevents streaming of neutrons to the experimental area, and it gives more room in the outer end of the beam tube, which is used to install collimator, shutters etc. The inner diameter of the thin part of the beam tubes must be D≥10 cm.

As seen from the discussion of the SORA-instruments a neutron moderator is necessary for all beam hole. In order to obtain the highest possible intensity, it should be placed as close to the reactor as possible. For the comparison we assumed that the neutron moderator could be placed in the stainless steel reflector at the interface to the blanket. It may only be possible to place one scatterer that close to the core. There is however the possibility of having more than one beam hole looking at the same neutron moderator.

One of these neutron moderators should be a cold source, probably a liquid hydrogen scatterer. It should be noted that due to the low mean power of SORA the installation of a cold scatterer is extremely simple.

There must be possibilities to insert and remove these neutron moderators, preferably through a vertical or near vertical channel which intercepts the beam channel as close to the reactor core as possible. The diameter of this channel must be larger than the diameter of the neutron moderator, probably at the order of 15 inner diameter.

In connection with the cold source a cooled beryllium filter is wanted to cut down the background from the zero power of the reactor. There must therefore exist possibilities for inserting such a filter, possibly together with the cold source. It may be noted that the length of this filter can be much smaller than usually used at a stationary reactor (~30 cm) because it only has to shield for the fast neutrons corresponding to P_{min}.

Vestibules in the reactor shield should be provided, if possible large enough to contain the background chopper discussed in 5.2.3.4.

5.4.2.- SPECIAL REQUIREMENTS.

a) Double chopper.

From the discussion on the double chopper it was seen to be essential to have the first chopper very close to the neutron source (50 cm from the source). The beam tube intended for double chopper instruments must therefore give possibilities for installation of the first chopper into the reactor shield. This requires a channel of 15-20 cm inner diameter which intercepts the beamtube at right angles at a distance of ~ 50 cm from the neutron moderator. It would be most convenient if this channel would be either horizontal or vertical (vertical is preferred).

b) Rotating crystal spectrometer.

There are no special requirement from this instrument.

c) Fast chopper.

Here we have the special requirements that the direction of the beamhole must allow a 1 km flight path.

5.4.3.- SPECIAL BEAM TUBE.

Experience from other reactors shows that tangential beam holes often are extremely useful due to their very low background (of neutrons as well as γ-rays). Therefore a tangential beam tube should, if possible be installed in the SORA reactor, even if it could only be used when other experiments (for instance measurements in the thermal column) are not being performed. With such a beam tube (which should have an inner diameter of about 15 cm) it would be possible to study for instance the time or energy distribution of secondary radiation caused by fast or slow neutrons.

A P P E N D I X I

FLUX DEPRESSION DUE TO COLD SOURCE IN THE VERY HIGH FLUX REACTOR

The cold source (liquid hydrogen) placed in the D_2O- reflector of the Very High Flux Reactor causes a flux depression which we will try to estimate here.
For this purpose we assume that the cold scatterer is a spherical shell of radius R and thickness t ($t \ll R$).

The number of neutrons absorbed in the H_2O is (see fig. 3)

$$\Sigma_{a_1} 4\pi R^2 t \bar{\phi}_1$$

The boundray condition at the interface is

$$4\pi R^2 D_2 (\text{grad}\phi_2)_R = 4\pi R^2 D (\text{grad}\phi_1)_R = 4\pi R^2 \Sigma_{a_1} t \bar{\phi}_1$$

The average flux in the light water layer is

$$\bar{\phi}_1 \approx \phi_1(R) - (\text{grad}\phi_1)_R \frac{t}{2}$$

or

$$\phi_1(R) \cong \bar{\phi}_1 + \frac{t}{2} \frac{\Sigma_{a_1} t \bar{\phi}_1}{D_1}$$

because the water layer is thin.

If we assume no absorption in the D_2O and the source far away we have in spherical geometry

$$D_2\, 4\pi r^2\ \operatorname{grad}\phi_2(r) = D_2\, 4\pi R^2\ (\operatorname{grad}\phi_2)_R$$

or

$$\operatorname{grad}\phi_2(r) = \frac{R^2}{r^2}\ \frac{\Sigma_{a,t}\,\bar{\phi}_1}{D_2}$$

Integrating this from $r = R$ to $r \to \infty$ we get

$$\int_{r=R}^{\infty} \operatorname{grad}\phi_2(r)\,dr = \phi_o - \phi_1(R) = \frac{R^2}{R}\ \frac{\Sigma_{a,t}\,\bar{\phi}_1}{D_2}$$

$$\phi_o - \bar{\phi}_1 - \frac{t}{2}\ \frac{\Sigma_{a,t}\,\bar{\phi}_1}{D_1} = R\ \frac{\Sigma_{a,t}\,\bar{\phi}_1}{D_2}$$

$$\frac{\phi_o}{\bar{\phi}_1} = 1 + \Sigma_{a,t}\left(\frac{t}{2D_1} + \frac{R}{D_2}\right)$$

with

R	=	10 cm
$\Sigma_{a,1}$	=	0,0017 cm^{-1}
t	=	1 cm
D	=	0,142 cm
D	=	0,80 cm

we get

$$\frac{\phi_o}{\bar{\phi}_1} = 1 + 0{,}017\ (3{,}52 + 12{,}5) = 1{,}27$$

This flux depression is hardly significant for our comparisons.

This value is even an upper limit, since we assumed no distributed source. In reality the hydrogen scatterer is placed in the reflector maximum. This means that we have a distributed source and therefore ϕ_o is reached rather close to the hydrogen scatterer.

A P P E N D I X I I

THERMAL NEUTRON PULSE FROM S O R A

This appendix gives the shape and intensity of the thermal neutron pulses obtained from a neutron moderator placed in the fast pulsed reactor "SORA".

The result of a calculation performed by Quiquemelle of the neutron flux in the thermal and the lowest epithermal neutron group for the SORA-reactor operating at 120 MW constant power is given in fig. 4 (curve a and b). The idealized geometry used in this calculation is also given in fig. 4.

The differential equation governing the thermal flux in the water moderator is the following :

$$D\nabla^2 \phi(r,t) - \Sigma_a \phi(r,t) + S(r,t) = \frac{1}{v} \frac{\partial \phi(r,t)}{\partial t}$$

Let us assume that the source is

$$S(r,t) = \begin{cases} R(r) & \text{for} \quad 0 \leq t \leq w \\ 0 & \text{for} \quad w \leq t \end{cases}$$

The source distribution R (r) is proportional to the epithermal flux shown in fig. 4. (curve a), and is constant in time.

The flux distribution $\phi(r, t)$ is a function of time. For small t, it is proportional to R (r) (curve a) but it approaches the thermal flux distribution shown in curve b for increasing time.

Before it reaches this distribution, the source is removed and the thermal flux will start to decay, changing its shape to approach a $\frac{1}{r}\cos(Br + \alpha)$ function (curve c).

In order to be able to solve the differential equation easily, we will have to neglect, that the thermal flux changes its shape with time. This is the same as assuming that the flux distribution and the source distribution is always proportional.

According to the flux shape considerations above, this approximation may not be too bad. We can check it later by comparing the flux distribution it leads to, with the actual flux distribution for the reactor at constant power (curve b, Fig. 4.).

Inserting

$$\varphi(r,t) = R(r)\,\varphi(t)$$
$$S(r,t) = R(r)\,s(t)$$

in the differential equation we get :

$$D\,\frac{\nabla^2 R(r)}{R(r)} - \Sigma_a + \frac{s(t)}{t} = \frac{1}{v}\,\frac{\frac{d\varphi(t)}{dt}}{\varphi(t)}$$

where we have separated the variables. We must therefore have

$$-\left(DB^2 + \Sigma_a\right)\varphi(t) + s(t) = \frac{1}{v}\,\frac{d\varphi(t)}{dt}$$

$$\nabla^2 R(r) + B^2 R(r) = 0$$

where B is a constant.

For the source considered here the solution is

$$\phi(r,t) = \begin{cases} Cvt_d\,\dfrac{\cos(Br +)}{r}\,\left(1 - \exp\left(t/t_d\right)\right) & 0 \leq t \leq w \\ Cvt_d\,\dfrac{\cos(Br +)}{r}\,\left(1 - \exp(-w/t_d)\right)\exp\left(-(t-w)/t_d\right) & w \leq t \end{cases}$$

where C is an integration constant and $t_d = \frac{1}{v(DB^2 + \Sigma_a)}$

For the reactor at constant power we get (infinite pulsewidth of the reactor)

$$\phi(r,t) = Cvt_d \frac{\cos(Br + \alpha)}{r}$$

This has to match curve b on fig. 4.

The following values for the constants

$$B = 0{,}379\ cm^{-1},\ D = 0{,}142\ cm,\ \Sigma_a = 0{,}017\ cm^{-1}$$

give extremely good agreement as shown in fig. 4. (curves b and c)

With these values we get

t_d = [illegible] sec

and

$Cv = 7.85\ 10^{20}$

The thermal flux at the position where it is maximum ($r \sim 16$ cm) is plotted in fig.5 as a function of time for two values of the reactor pulse width w (50 /usec and 25 /usec). The fact is used that the number of neutrons in the reactor pulse is the same in the two cases. It is seen that the thermal flux is very insensitive to variations of the reactor pulse widths in the region of interest.

With a pulse width 25 /usec $\leq w \leq$ 50 /usec the average thermal flux is about $1.9 \times 10^{15}\ \frac{n}{cm^2\ sec}$. It does not vary much for averages taken over times from 10 to 50 /usec. (corresponding to the accepted pulse width of the instruments discussed in chapter 2).

However, in order to make use of this thermal flux for beam experiments, we must have a re-entrant channel to the center of the moderator. The size of this channel ($\sim 50 cm^2$ cross section) is quite large compared to

the thickness of the moderator (7cm), so that the flux depression will not be negligible. Let us therefore estimate, that the thermal flux available for beam experiments is

$$\Phi_{th} \approx 1 \times 10^{15} \quad \frac{n}{cm^2 \, sec}$$

We have assumed so far that the water scatterer surrounds the whole core. In the actual case it will be finite and t_d will therefore be somewhat smaller than the 120 µsec (as calculated above). Fig.6 shows the maximum flux as a function of t_d for two values of w (25 and 50 µsec). It is seen that the loss of intensity due to leakage and absorption is not too large as long as the diffusion time t_d is more than twice the reactor pulse length w. A consequence of this is that the shorter the reactor pulse w is, the larger leakage can be permitted.

NOTE

The problem of the thermal neutron pulse has been recalculated by Asaoka (to be published). He applied a multiple collision method to a plane infinite slab geometry.

As source distribution the exact curve "a" of fig . 4 has been chosen and no assumption on the flux distribution were made. In this way t_d and the average neutron density were calculated. The slightly lower t_d ($\approx$ 100 μsec), he obtains, may be understood from geometry reasons. The maximum flux if a cosine distribution is assumed, is estimated to be 2.0×10^{15} n cm^{-2} sec^{-1}, which coincides with our value, since the peak flux is not very sensitive to t_d (fig.6).

REFERENCES

The present study was initiated by the development of the SORA reactor under the direction of V.Raievski.

The type of beamhole experiments was suggested by W.Kley.
The neutron flux data were calculated by Quiquemelle (to be published), with a one dimensional S_n code for 18 energy groups.

The reactor characteristics for table 9 are taken from R.Misenta and G. Di Cola internal report Euratom-Ispra-454 (1963).

For comparison with other high performance instruments see : Egelstaff, Cooking and Alexander, AECL - 1494, and Poole (Talk at Harwell 11/7/1962), communicated to us by S.J.Cooking and R.D. Lowde. The thermal flux of the V ry High Flux Reactor is taken from : Halliday and Wade : ENEA Symposium, Harwell, July 1962. ($2 \times 10^{15} \frac{n}{cm^2 \, sec}$ at 100 MW).

LIST OF FIGURES

L I S T O F T A B L E S

$r = 5$ cm, $l_1 = 400$ cm, $l_2 = l_3$ $\alpha_3 = 5 \times 10^{-2}$
$F_2 = 43$ cm^2 for $s = 0.30$ cm;
$F_2 = 37.5$ cm^2 for $s = 0.15$ cm (see fig.1,2),
$\varepsilon = 1.0$

Table 6 Comparison of SORA and VHFR for experiments with cold neutrons (Be-filter), for 2 different mean powers of the SORA.

Table 7 Operating characteristics of a 4 rotor type spectrometer at the VHF reactor for thermal neutron experiments.
$R = 12.7$ cm, $l_1 = 400$ cm, $l_2 = l_3$, $\alpha_3 = 5 \times 10^{-2}$
$F_2 = 6.1$ cm^2 (see fig. 1, the fast neutron rotors are left out)
$\varepsilon = 1.0$

Table 8 Comparison of SORA and VHFR for experiments with thermal and epithermal neutrons, for 2 different mean powers of SORA.

Table 9 Characteristic data for the SORA performance.

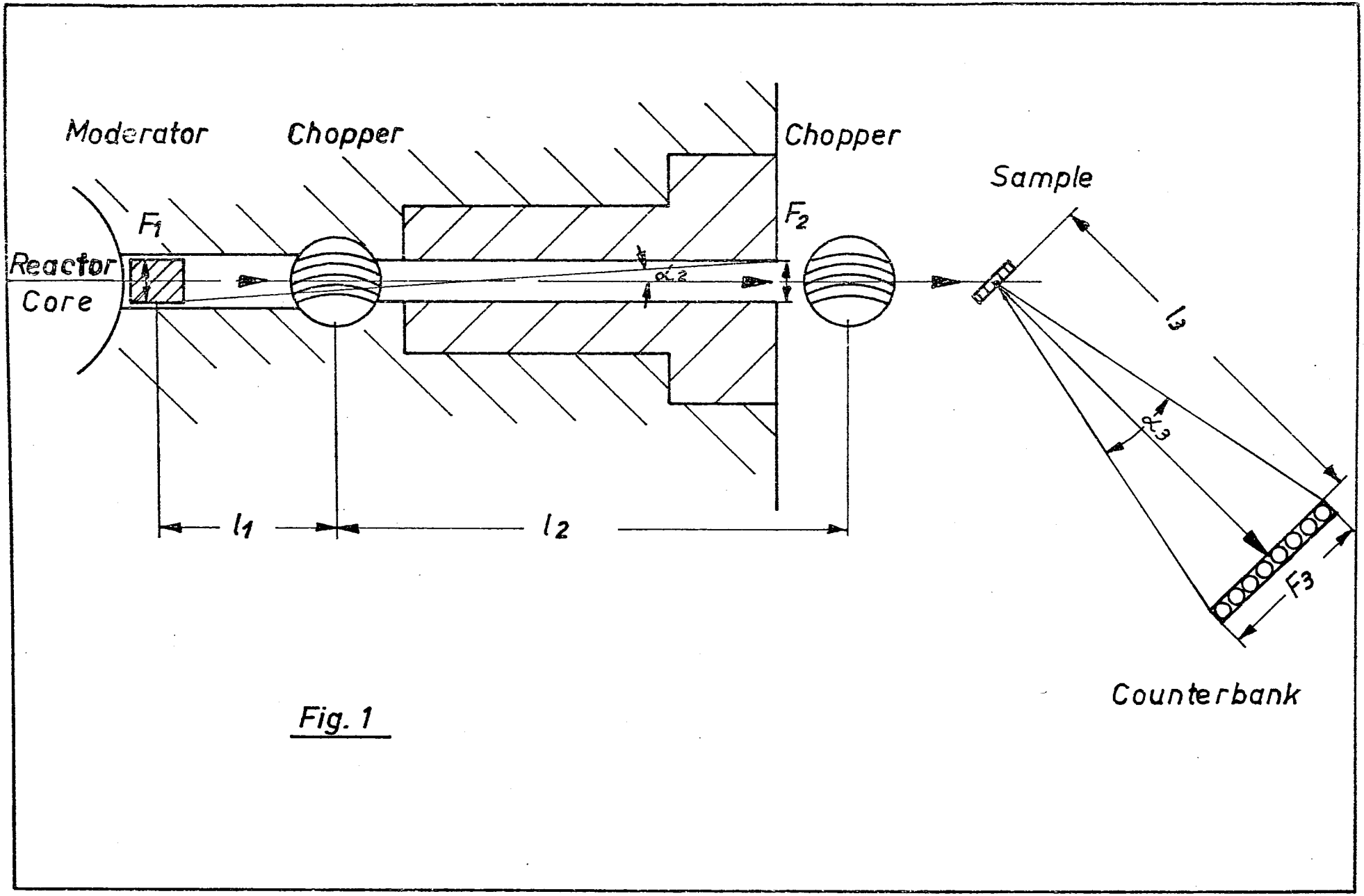
Moderator
Chopper
Chopper
Sample
F1
F2
Reactor
Core
l1
l2
l3
F3
Counterbank

Fig. 1

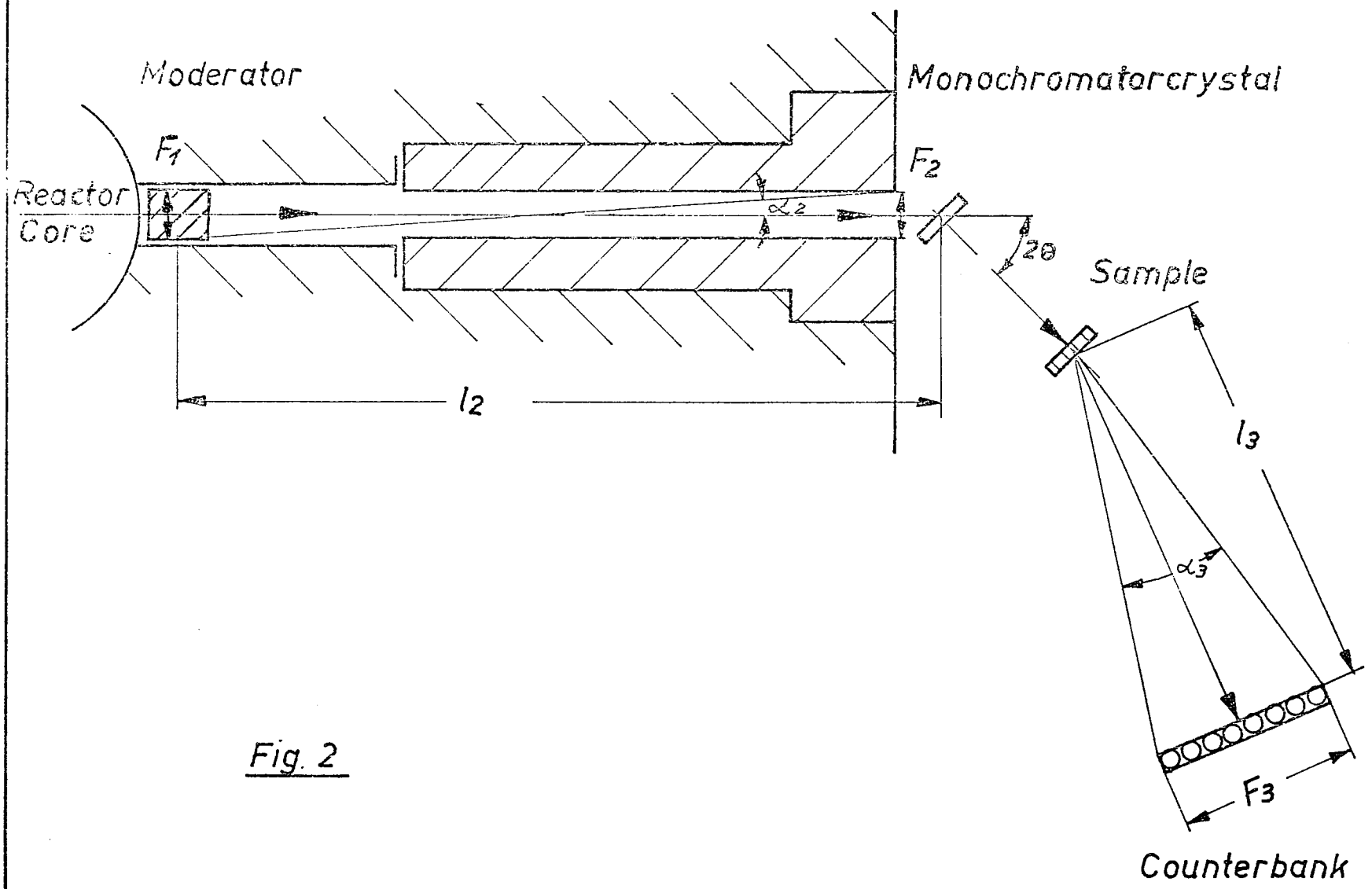
Moderator
Monochromatorcrystal
F1
F2
Reactor
Core
α2
2θ
Sample
l2
l3
α3
F3
Counterbank

Fig. 2

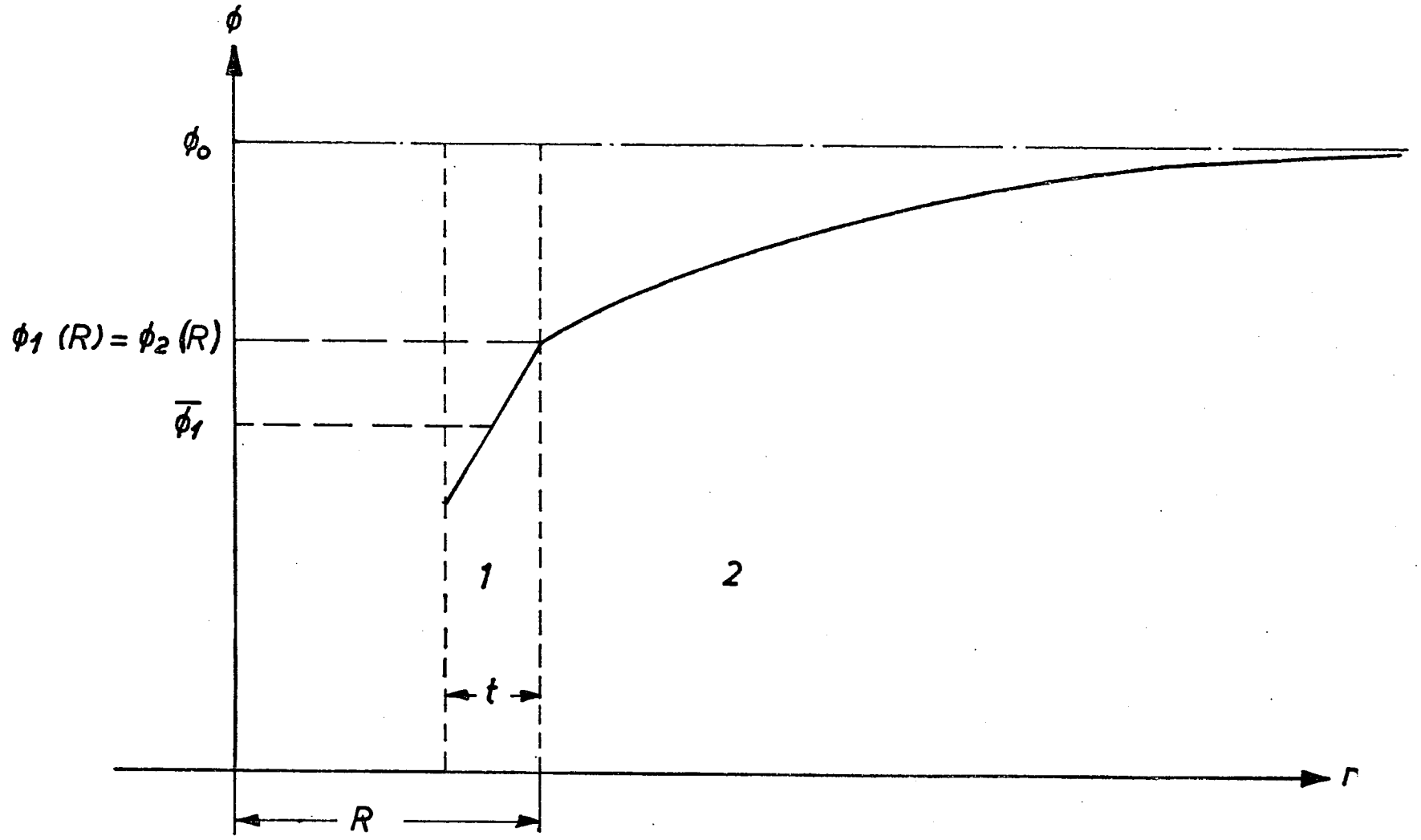

Fig. 3

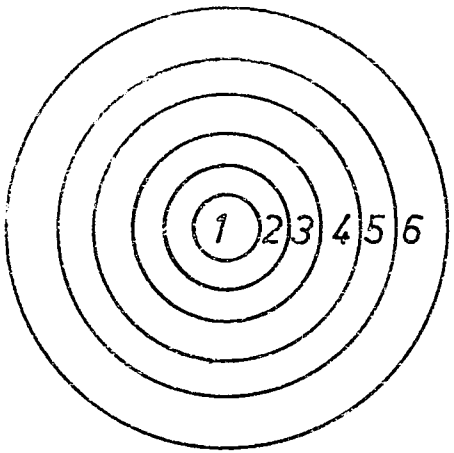

1 Core
2 Blanket
3 H_2O-moderator
4 Stainless steel
5 Lead
6 Aluminum

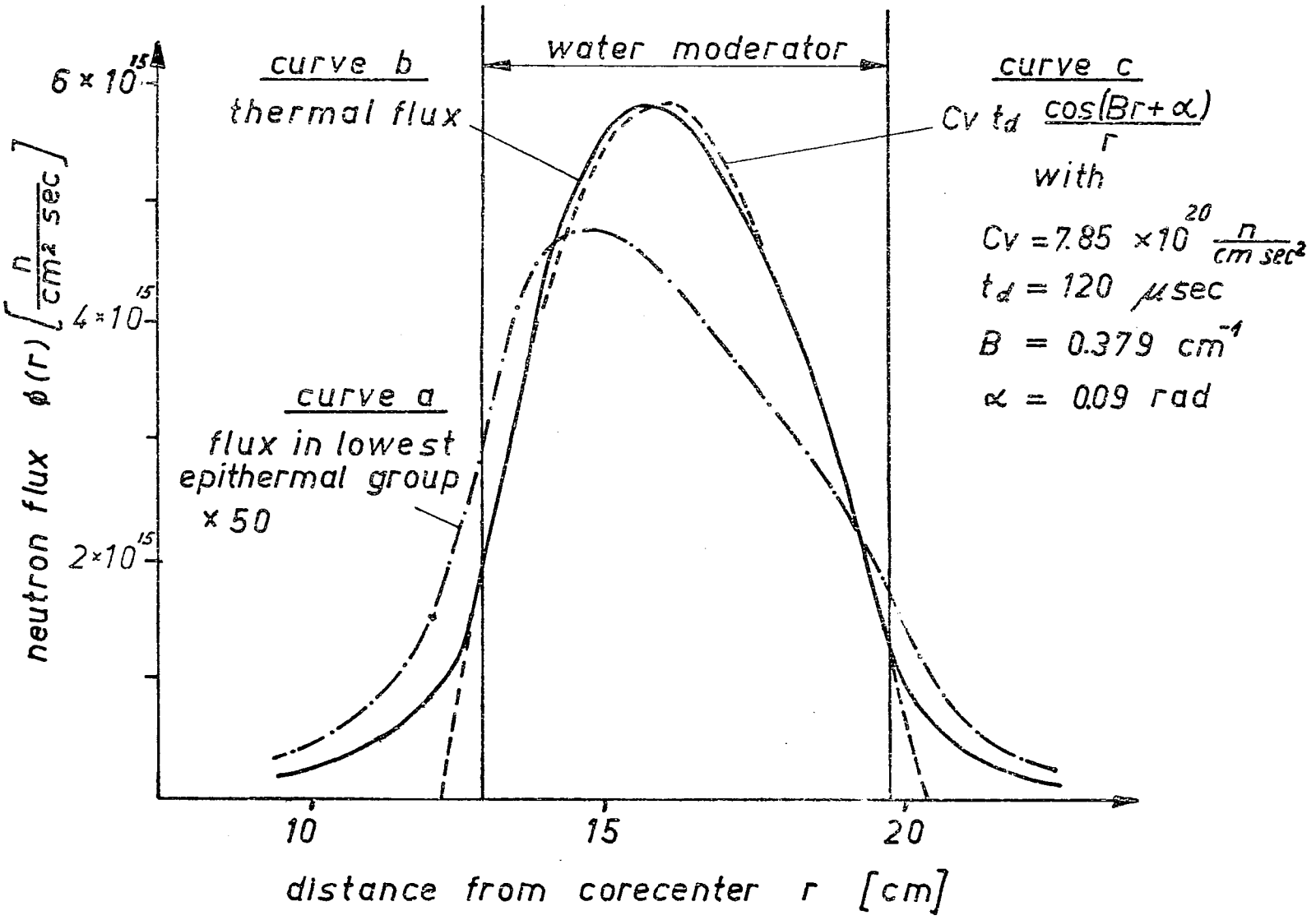

Fig. 4

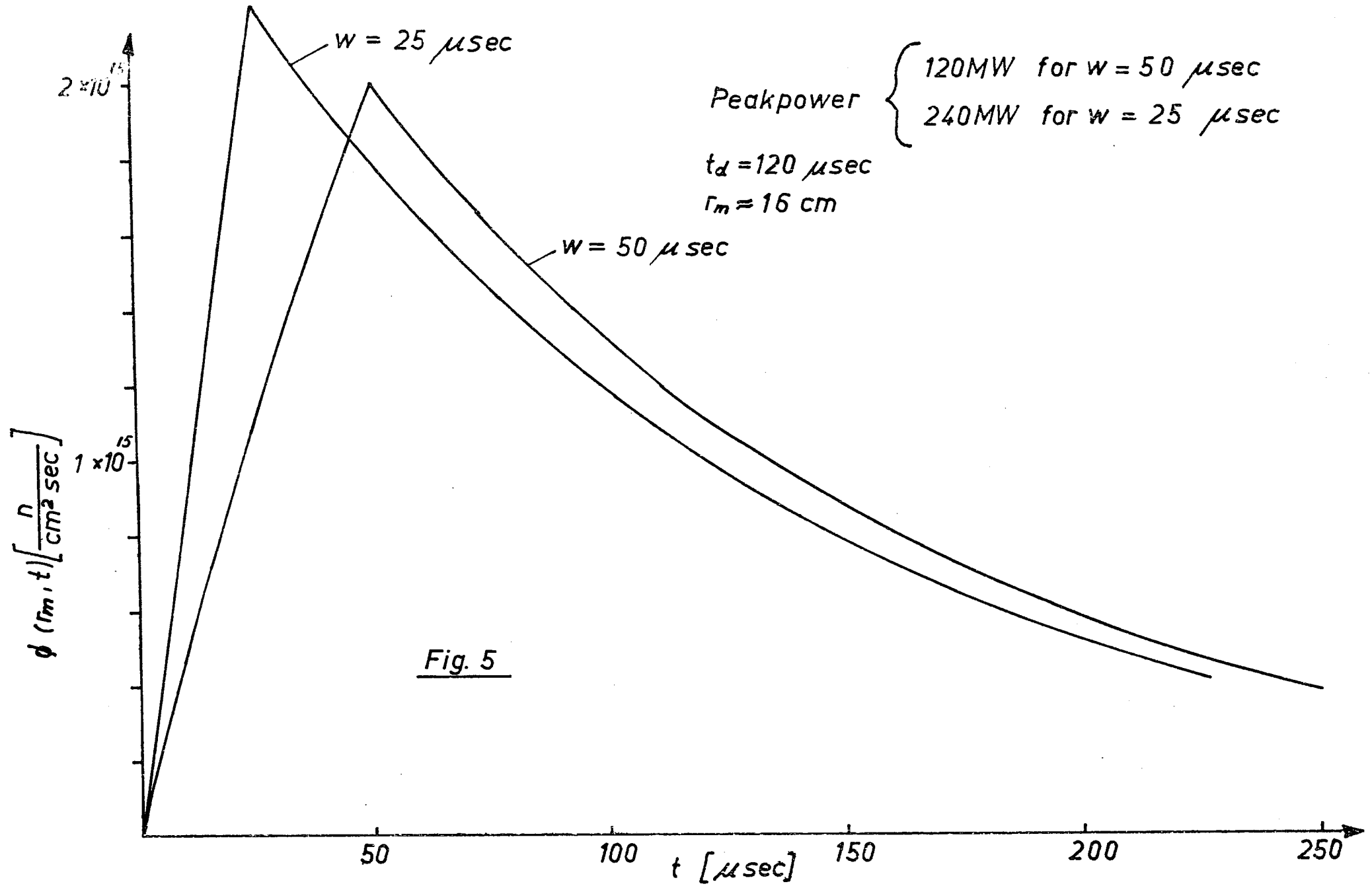
w = 25 μsec
w = 50 μsec
Peakpower
120MW for w = 50 μsec
240MW for w = 25 μsec
t_d = 120 μsec
r_m = 16 cm
2×10^{15}
1×10^{15}
$\phi(r_m, t)\left[\frac{n}{cm^2 sec}\right]$
50
100
150
200
250
t [μsec]

Fig. 5

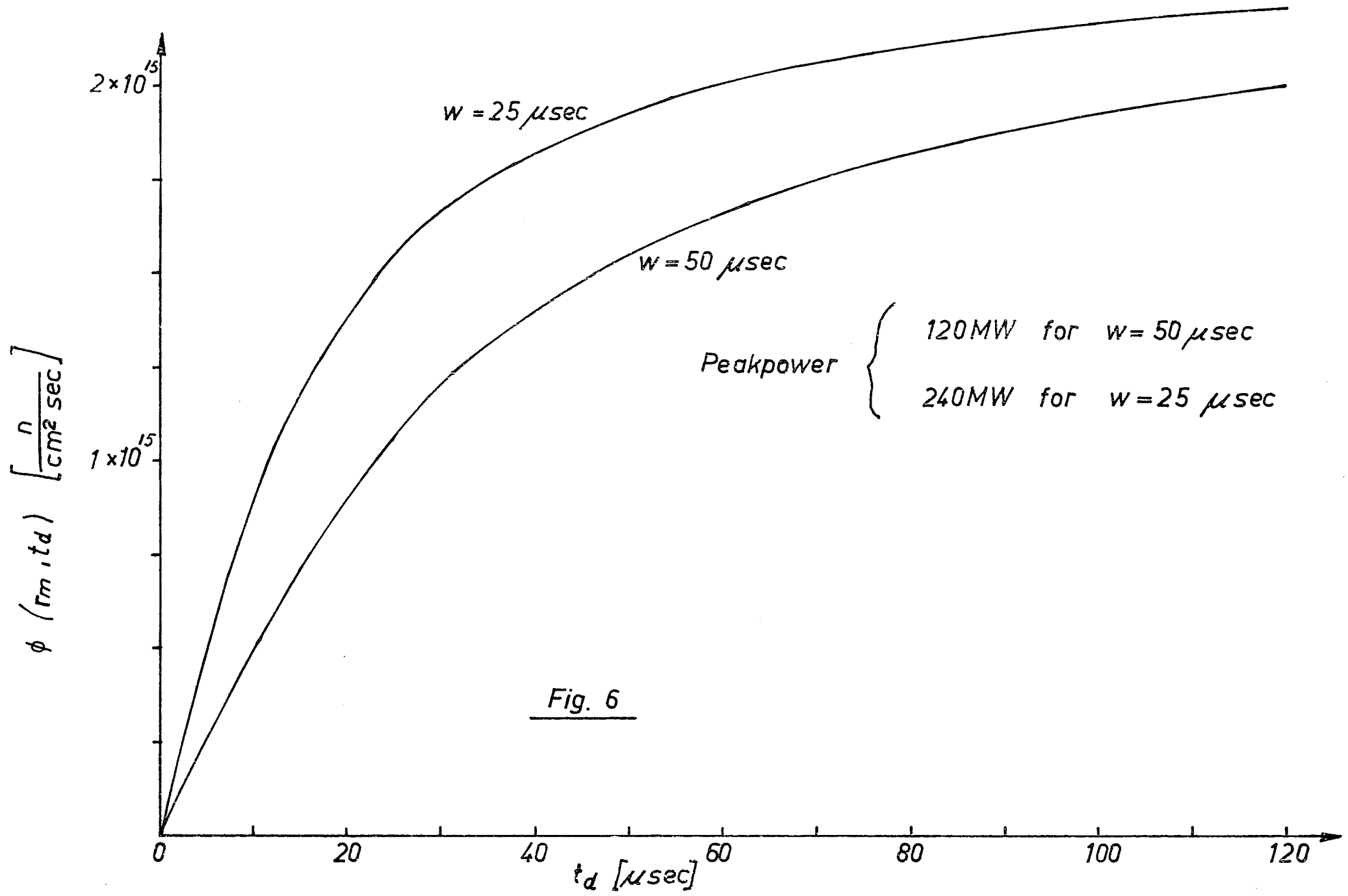
2×10^15
1×10^15
w = 25 μsec
w = 50 μsec
Peakpower
120MW for w = 50 μsec
240MW for w = 25 μsec
φ (rm , td) [n/cm² sec]
0
20
40
60
80
100
120
td [μsec]

Fig. 6

Table 1

v [m/sec]	500				1000			
s [cm]	0,30	0,30	0,30	0,30	0,30	0,30	0,30	0,15
ϱ [cm]	79,6	39,8	39,8	19,9	79,6	39,8	39,8	39,8
β	1,9	0,95	0,95	0,47	1,9	0,95	0,95	0,47
ν [sec^{-1}]	50	100	100	200	100	200	200	200
l_2 [cm]	150	150	300	300	150	150	300	300
α_2 [rad]	0,033	0,033	0,017	0,017	0,033	0,033	0,017	0,017
t_2 [μsec]	3000	3000	6000	6000	1500	1500	3000	3000
Δt [μsec]	96	48	48	24	48	24	24	12
Δt_s [μsec]	104	52	26	13	52	26	13	13
$\Delta E_1 / E_1$	0,13	0,06	0,022	0,011	0,13	0,06	0,022	0,016
$\Delta E_2 / E_2$	0,09	0,05	0,016	0,008	0,09	0,05	0,016	0,008
$\frac{F_2^2}{4\pi l_2 (l_1 + l_2)}$	$4,9 \times 10^{-3}$	$4,9 \times 10^{-3}$	$1,4 \times 10^{-3}$	$1,4 \times 10$	$4,9 \times 10^{-3}$	$4,9 \times 10^{-3}$	$1,4 \times 10^{-3}$	$1,0 \times 10^{-3}$
$\frac{I_s}{\Phi(E_1)\,\Delta E_1}$	$1,2 \times 10^{-10}$	$6,0 \times 10^{-11}$	$1,7 \times 10^{-11}$	$8,4 \times 10^{-12}$	$6,0 \times 10^{-11}$	$3,0 \times 10^{-11}$	$8,4 \times 10^{-12}$	$3,0 \times 10^{-12}$

Table 2

v [m/sec]	2000				4000			
s [cm]	0,30	0,30	0,15	0,15	0,30	0,15	0,10	0,10
ϱ [cm]	79,6	79,6	79,6	79,6	159,2	159,2	159,2	159,2
β	1,9	1,9	0,95	0,95	3,8	1,9	1,3	1,3
ν [sec^{-1}]	200	200	200	200	200	200	200	200
l_2 [cm]	150	300	300	600	300	300	450	600
α_2 [rad]	0,033	0,017	0,017	0,008	0,017	0,017	0,013	0,008
t_2 [μsec]	750	1500	1500	3000	750	750	1125	1500
Δt [μsec]	24	24	12	12	24	12	8	8
Δt_s [μsec]	26	13	13	6	13	13	9	7
$\Delta E_1/E_1$	0,13	0,045	0,032	0,011	0,09	0,064	0,028	0,020
$\Delta E_2/E_2$	0,09	0,032	0,023	0,008	0,064	0,045	0,020	0,014
$\frac{F_2^2}{4\pi l_2 (l_1 + l_2)}$	$4,9 \times 10^{-3}$	$1,4 \times 10^{-3}$	$1,0 \times 10^{-3}$	$2,9 \times 10^{-4}$	$1,4 \times 10^{-3}$	$1,0 \times 10^{-3}$	$3,8 \times 10^{-4}$	$2,2 \times 10^{-4}$
$\frac{I_3}{\phi(E_1)\,\Delta E_1}$	$3,0 \times 10^{-11}$	$8,4 \times 10^{-12}$	$3,0 \times 10^{-12}$	$8,7 \times 10^{-13}$	$8,4 \times 10^{-12}$	$3,0 \times 10^{-12}$	$7,6 \times 10^{-13}$	$4,4 \times 10^{-13}$

Table 3

θ	2θ	$ctg\,\theta$	$ctg\,\theta\,\Delta\theta$	$\frac{\lambda}{d}=2\sin\theta$	v_n [m/sec] ($d=2$ Å)	v_n [m/sec] ($d=1{,}5$ Å)	v_n [m/sec] ($d=1{,}0$ Å)
63°	126°	0,5	0,25 %	1,79	1100	1470	2220
45°	90°	1	0,5 %	1,41	1400	1870	2810
26,5°	53°	2	1,0 %	0,89	2220	2960	4450
18°	36°	3	1,5 %	0,62	3200	4250	6380
14°	28°	4	2,0 %	0,484	4100	5460	8200
11,3°	22,6°	5	2,5 %	0,392	5050	6750	10100
9,5°	19°	6	3 %	0,330	6000	8000	—
8,1°	16,2°	7	3,5 %	0,282	7000	9360	—
7,1°	14,2°	8	4 %	0,247	8000	—	—

Table 4

$v_2 = v_3$ [m/sec]	1000		2000			4000			8000	
$\frac{\Delta E_2}{E_2}$	0,05	0,025	0,05	0,025	0,010	0,05	0,025	0,010	0,05	0,025
2ϑ	$\approx 90°$	$\approx 90°$	$\approx 90°$	$\approx 90°$	$\approx 90°$	$\geqslant 36°$	$\geqslant 36°$	$\geqslant 53°$	$> 22,6°$	$> 22,6°$
$\frac{\Delta\vartheta}{\alpha}$	1	0,5	1	0,5	0,20	0,33	0,167	0,1	0,2	0,1
$tg\vartheta$	1	1	1	1	1	0,326	0,326	0,5	0,2	0,2
$\frac{\Delta E_3}{E_3}$	0,05	0,025	0,05	0,025	0,010	0,05	0,025	0,01	0,05	0,025
Δt [μsec]	100	50	50	25	10	25	12,5	5	12,5	6,3
n [rpm]	2500	2500	5000	5000	5000	3330	3330	5000	4000	4000
$\frac{I_3}{\phi(E)\Delta E}$	$1,6\times10^{-11}$	4×10^{-12}	8×10^{-12}	2×10^{-12}	$3,2\times10^{-13}$	$1,3\times10^{-12}$	$3,3\times10^{-13}$	8×10^{-14}	4×10^{-13}	1×10^{-13}

Table 5

v [m/sec]	500				1000			
s [cm]	0,30	0,30	0,30	0,30	0,30	0,30	0,30	0,15
ϱ [cm]	79,6	39,8	39,8	19,9	79,6	39,8	39,8	39,8
β	1,9	0,95	0,95	0,48	1,9	0,95	0,95	0,48
ν [sec^{-1}]	50	100	100	200	100	200	200	200
l_2 [cm]	150	150	300	300	150	150	300	300
α_2 [rad]	0,0136	0,0136	0,0107	0,0107	0,0136	0,0136	0,0107	0,0107
t_2 [μsec]	3000	3000	6000	6000	1500	1500	3000	3000
Δt [μsec]	96	48	48	24	48	24	24	12
Δts [μsec]	44	22	17	8	22	11	8	8
$\Delta E_1/E_1$	0,091	0,045	0,023	0,011	0,091	0,045	0,023	0,011
$\Delta E_2/E_2$	0,064	0,032	0,016	0,008	0,064	0,032	0,016	0,008
$1 + A$	1,91	1,91	1,79	1,79	1,91	1,91	1,79	1,79
$\frac{F_2^2}{4\pi (l_1 + l_2)^2}$	$4,9 \times 10^{-4}$	$4,9 \times 10^{-4}$	$3,0 \times 10^{-4}$	$3,0 \times 10^{-4}$	$4,9 \times 10^{-4}$	$4,9 \times 10^{-4}$	$3,0 \times 10^{-4}$	$2,3 \times 10^{-4}$
$\frac{I_3}{\phi (E_1)\, \Delta E_1}$	$9,0 \times 10^{-11}$	$9,0 \times 10^{-11}$	$5,4 \times 10^{-11}$	$5,4 \times 10^{-11}$	$9,0 \times 10^{-11}$	$9,0 \times 10^{-11}$	$5,2 \times 10^{-11}$	$2,6 \times 10^{-11}$

Table 6

Comparison of SORA and VHFR for experiments with cold neutrons

v_n [m/s]	500				1000			
$\frac{\Delta E_1}{E_1} \approx \frac{\Delta E_2}{E_2}$ [%]	1	2.5	5	10	1	2.5	5	10
$\left(\frac{\text{Intensity VHFR - instr.}}{\text{Intensity SORA - instr.}}\right)_1$	13	6.5	3	1.5	18	12.5	6	3
$\left(\frac{\text{Intensity VHFR - instr.}}{\text{Intensity SORA - instr.}}\right)_2$	5.2	2.6	1.2	0.6	7.2	5	2.4	1.2

1) $\bar{P} = 100$ kW

2) $\bar{P} = 250$ kW

Table 7

v [m/s]	2000				4000			
s [cm]	0,635	0,635	0,635	0,635	0,635	0,635	0,635	0,635
ϱ [cm]	106	53	26,5	26,5	106	53	53	53
β	0,83	0,42	0,21	0,21	0,83	0,42	0,42	0,42
ν [sec^{-1}]	150	300	600	600	300	600	600	600
l_2 [cm]	150	150	150	300	150	150	300	600
α_2 [rad]	0,0120	0,0120	0,0120	0,0094	0,0120	0,0120	0,0094	0,0066
t_2 [μsec]	750	750	750	1500	375	375	750	1500
Δt [μsec]	26,4	13,2	6,6	6,6	13,2	6,6	6,6	6,6
Δt_s [μsec]	12,7	6,4	3,2	2,5	6,4	3,2	2,5	1,4
$\Delta E_1/E_1$	0,100	0,050	0,024	0,012	0,100	0,050	0,024	0,012
$\Delta E_2/E_2$	0,070	0,035	0,017	0,009	0,070	0,035	0,017	0,009
$(1+A)^2$	7,3	7,3	7,3	5,1	7,3	7,3	5,1	2,77
$\frac{F_2^2}{4\pi (l_1 + l_2)^2}$	$9{,}80\times10^{-6}$	$9{,}80\times10^{-5}$	$9{,}80\times10^{-6}$	$6{,}05\times10^{-6}$	$9{,}80\times10^{-6}$	$9{,}80\times10^{-6}$	$6{,}05\times10^{-6}$	$2{,}96\times10^{-6}$
$\frac{I_э}{\phi(E_1)\Delta E_1}$	$5{,}7\times10^{-12}$	$5{,}7\times10^{-12}$	$5{,}7\times10^{-12}$	$2{,}5\times10^{-12}$	$5{,}7\times10^{-12}$	$5{,}7\times10^{-12}$	$2{,}5\times10^{-12}$	$6{,}5\times10^{-13}$

Table 8

Comparison of SORA and VHFR for experiments with thermal and epithermal neutrons

v_n [m/s]	2000				4000			
$\frac{\Delta E_1}{E_1} \approx \frac{\Delta E_2}{E_2}$ [%]	1	2.5	5	10	1	2.5	5	10
$\left(\frac{\text{Intensity VHFR-instr.}}{\text{Intensity SORA-instr.}}\right)_1$	5.7	3.8	1.3	0.4	3	6.5	3.8	1.3
$\left(\frac{\text{Intensity VHFR-instr.}}{\text{Intensity SORA-instr.}}\right)_2$	2.3	1.5	0.5	0.16	1.2	2.6	1.5	0.5

1) $\bar{P}$ = 100 kW

2) $\bar{P}$ = 250 kW

Table 9

SORA characteristics

ν_r [sec^{-1}]	w [μsec]	$p = \frac{P_{max.}}{P_{min.}}$	w [μsec]	$p = \frac{P_{max.}}{P_{min.}}$	$f_{th.}$
10	46	8250	23	16500	2060
12,5	46	6200	23	12400	1550
25	48	3050	24	6100	760
50	51	1400	25	2800	350
100	53	625	26	1250	156
	report Ispra 454 (1963)		tentative data		